Technical Note

Analytical Study of Interior Rigid Bents Arrangement on Seismic Response of Tall Buildings

Masoud Azhdarifar[1], Afshin Meshkat-Dini[2*], and Abdol-Reza Sarvghad Moghadam[3]

1. M.Sc. Graduate, Kharazmi University, Faculty of Engineering, Tehran, Iran
2. Assistant Professor, Kharazmi University, Faculty of Engineering, Tehran, Iran,
* Corresponding Author; email: meshkat@khu.ac.ir
3. Associate Professor, International Institute of Earthquake Engineering and Seismology (IIEES), Tehran, Iran

Received: 19/08/2016
Accepted: 01/05/2017

ABSTRACT

In this research, the performance abilities associated with tube type lateral load resistant framed systems are studied in order to assess the seismic response parameters of steel tall buildings under both far and near-field records. For this purpose, four 30 story structural models with separated framed tube-based skeletons were selected and designed. The structural models have been designed according to the Iranian seismic code 2800 (4th edition). The structural response parameters have been computed and obtained by conducting a number of non-linear dynamic time history analyses. Based on the analytical results obtained from nonlinear analyses, the values of maximum inter-story drift, story acceleration and velocity, dynamic base shear, configuration of plastic hinges mechanism, shear lag phenomena and residual drift were assessed and investigated. Yet, the results have been discussed and compared with the "life safety" and "collapse prevention" performance limits, as recommended by FEMA 356. Findings from this study reveal that mean maximum demands and the dispersion in the peak values were considerably higher for near-fault records than far-fault motions. The obtained results indicate the fact that an appropriate arrangement and bundled configuration of interior rigid frames could remarkably reduce the appearance of shear lag phenomenon almost up to 70% as compared to the corresponding results with basic framed tube.

Keywords:
Non-linear dynamics; Steel skeleton; Framed tube; Strong ground motion; Velocity pulse

1. Introduction

Assessments of structural damages during strong earthquakes such as Loma Prieta 1989, Northridge 1994, Kobe 1995 in Japan, Chi-Chi 1999 in Taiwan, Tabas 1978 and Bam 2003 in Iran indicate the entire destructive influences of powerful near-fault records [1-3].

One of the most common issues in engineering seismology is the evaluation of the physical characteristics of strong ground motions in near-fault zones and their effects on the performance of specific structures especially medium to high-rise buildings [4-7].

An efficient structural skeleton used in the construction of medium to high-rise buildings is called rigid tube or framed tube system. Generally, a framed tube skeleton can be defined as a three-dimensional system that provides very stiff structural bents, forming a "tube type skeleton" around the perimeter

of the building. This system's behavioral nature is in a way more complicated than the performance of a pure solid tube-type framework. This concept is approved in regards to the combined shear-flexure behavior of framed tube structures [8-9].

The aspect ratio of casements is affected by girder section height and the column element width. In the case of lateral load effects at the lower floors, especially at the ground level, the axial force in the corner columns is much larger than that of the center column of the flange frames. This can be due to the flexibility of the spandrel beams that imposes the shear lag effects; therefore, the axial stress resultants in the corner columns should be greater than that of the inner columns of the web frames as shown in Figure (1) [10-12]. Attending to subjects and concepts of the engineering design of framed-tube structures and a thorough understanding of the dynamic behavior of their major skeletal elements, which consist of deep girders and large-section columns, would help optimize the seismic behavior of these structures. Based on this fact, it is necessary to be more careful in structure plan geometry, span dimension as well as the configuration of rigid frames in the architectural plan of framed-tube [13-15].

It is considerable that having a decent distribution of inner rigid bents configuration in framed tube-type structures, can lead to a more eligible distribution of axial forces in the perimeter columns of the plan. In addition, this structural phenomenon can reduce the dynamic shear lag effects almost up to 75% and 70% respectively in seismic performance of two structural systems such as multi-cell and bundled tubes. This is more evident as compared to the corresponding results of basic framed tube skeleton.

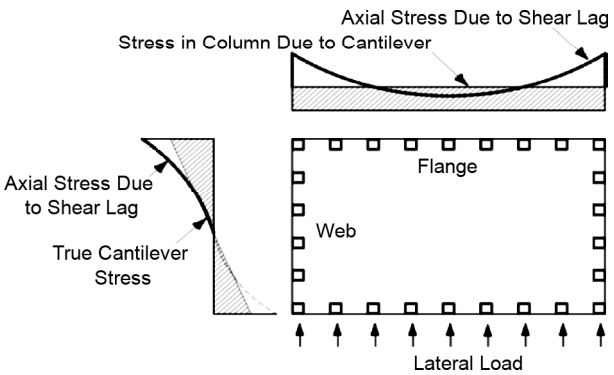

Figure 1. Axial stress distribution in the columns of the framed tube structure in web and flange panels [11].

2. Pulse-Like Ground Motions

One of the most distinctive characteristics of near-field records is the capability to produce both powerful short-term and long-term velocity pulses along with strong acceleration spikes in the velocity time history [16-18]. This is an important factor to differentiate between these types of records and those of far-field zones shown in Figure (2-a and b).

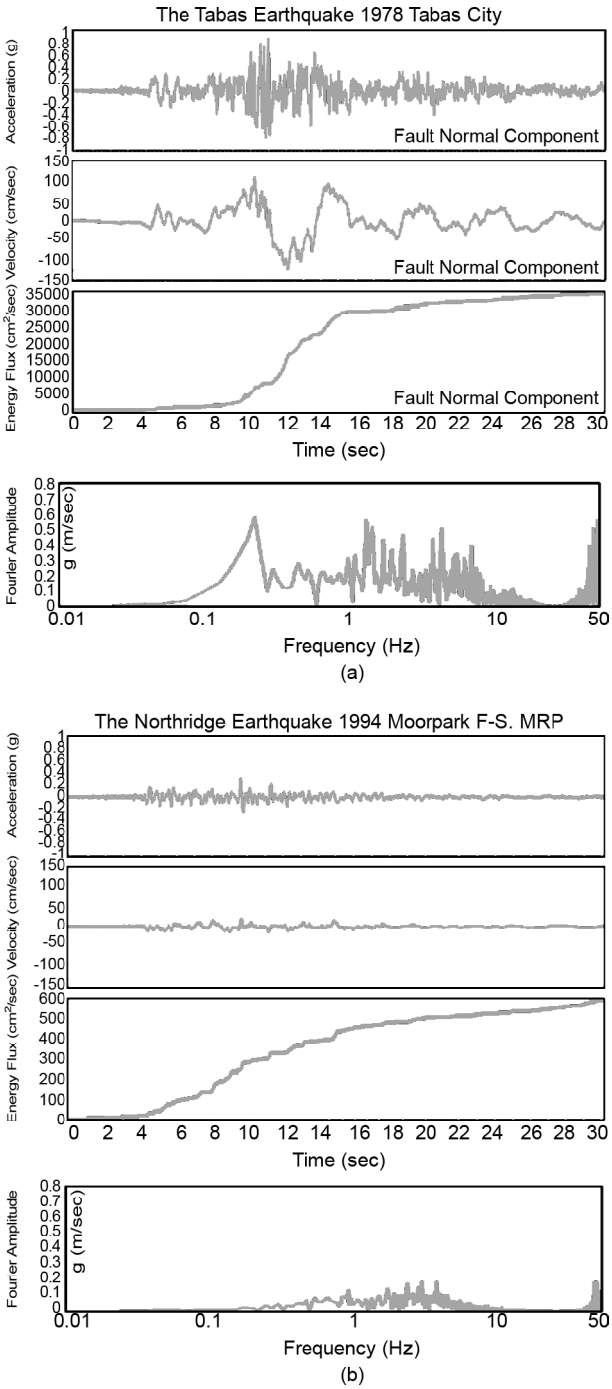

Figure 2. The physical and spectral characteristics of two selected records (a) The near-fault ground motion with forward directivity effects of Tabas 1978, (b) The far-fault ground motion of Moor Park 1994 (MRP), [11].

Much evidence of such effect as a basic attribute of near-field ground motions, has been reported in recent destructive earthquakes of 1978 Tabas, Iran; 1995 Kobe, Japan; 1999 Chi-Chi, Taiwan; 2003 Bam, Iran; and 2009 L'Aquila, Italy [19-20].

The presence of pulse-like features in the time history of near-field records causes the input kinetic energy of these movements to be many times larger than those in far-field records as displayed in Figures (2-a and b). The effects of earthquake records containing velocity pulses on engineering structures performance have been pointed out by several researchers [21-22]. However, the records affected by backward-directivity faulting process typically do not exhibit any obvious and great pulse-like features. Most of the kinetic energy related to powerful earthquake records with forward-directivity effects is released during a short limited period within the pulse configuration [23]. Recently, Chioccarelli et al discussed the amplification of elastic and inelastic seismic demands for pulse-like fault-normal records of the 2009 L'Aquila, Italy earthquake versus the (T_1/T_p) [24-26].

Moreover, in the Fourier spectrum of these records, instead of the development of the maximum vertical axis components into a wide range of frequency domain (Figure 2-b), it is limited to a small range. Furthermore, sometimes even the distinct maximum vertical axis component would be revealed only at one particular frequency (Figure 2-a). As indicated by many strong records, the velocity-type vertical axis components resulting from the Fourier spectrum would have large amounts even when they correspond to higher modes of vibration of the structural system [27-28]. Therefore, in the assessment of the seismic behavior of medium-rise to tall buildings, it is important to pay attention accurately to the effects of the proximity of higher modes period especially for the basic torsional mode of vibration, to the corresponding vertical axis components obtained from the Fourier spectrum of a considered strong record [29-30].

The overall kinetic energy variation pertaining two records is also shown in Figure (2), in which the Tabas station is located near to the epicenter of the Tabas earthquake 1978 and the MRP station takes place in the far zone. According to Figure (2-a), about 90 percent of the kinetic energy of the near-field ground motion is released within less than 8 seconds [31]. This case for the El Centro 1940 record has a domain of near 24 seconds in which the releasing of the low-scale kinetic energy is more balanced and occurs in a longer range of time as shown in Figure (2-b) [32-33].

3. Description of the Studied Models

As mentioned in previous sections, this research presents the analytical assessment of the seismic response of four studied models (Figure 3). The first two models are framed tube and bundled tube structures respectively with full rigid beam-column connections. The third and fourth models which are the noted ones in this research are named castled tube and cellular tube, respectively. The studies conducted in this research follow the same analytical path and four companion structural models with different arrangement of internal rigid bents are chosen for a prototype 30-story steel building. All models are designed based on the concept of medium ductility level according to codified provisions of the Iranian seismic code 2800 (4th edition) and Iranian national building code (steel structures - division 10) [34-35].

All four studied models are considered regular and symmetric in the plan and height. The pale lines in the studied plans indicate pinned connection and the bold thick lines illustrate rigid connections of beams to columns. The period of the first three seismic modes of the studied models are shown in Table (1). It is a desirable criterion in the process of

Table 1. Modal vibration periods of structural models.

Lateral Resistant System	T_1 (sec) First Lateral Mode	T_2 (sec) Second Lateral Mode	T_3 (sec) Initial Torsional Mode
Framed Tube	4.47	2.62	1.67
Bundled Tube	3.70	2.62	1.39
Castled Tube	3.82	2.37	1.41
Cellular Tube	3.87	2.56	1.42

structure design that is witnessed in both X and Y directions of the structures in Figure (3). The section characteristics of girders and columns of the studied models in Figure (3) are represented in Table (2). In order for a detailed and parametric analysis of the dynamic shear lag effect, which is the main point of this recent study, the 30 story studied models were analyzed subjected to an ensemble of strong recorded ground motions.

In order to relatively control design stress ratio in all considered structural models and the developed version of framed tube skeletons, the effort is for the inner rigid frame arrangement to have structural order and harmony considering the number of beams and columns. Therefore, it is possible to assess and compare their resulting response parameters with the basic model of single framed tube. The following agreements are applied in the act of naming, so that mentioning each of these models would be easier and more comprehensible. The agreement is to use the F.T. index for the basic tube frame model, B.T. index for the bundled tube, Ca.T. index for the castled tube and finally, Ce.T. index for the cellular tube frame.

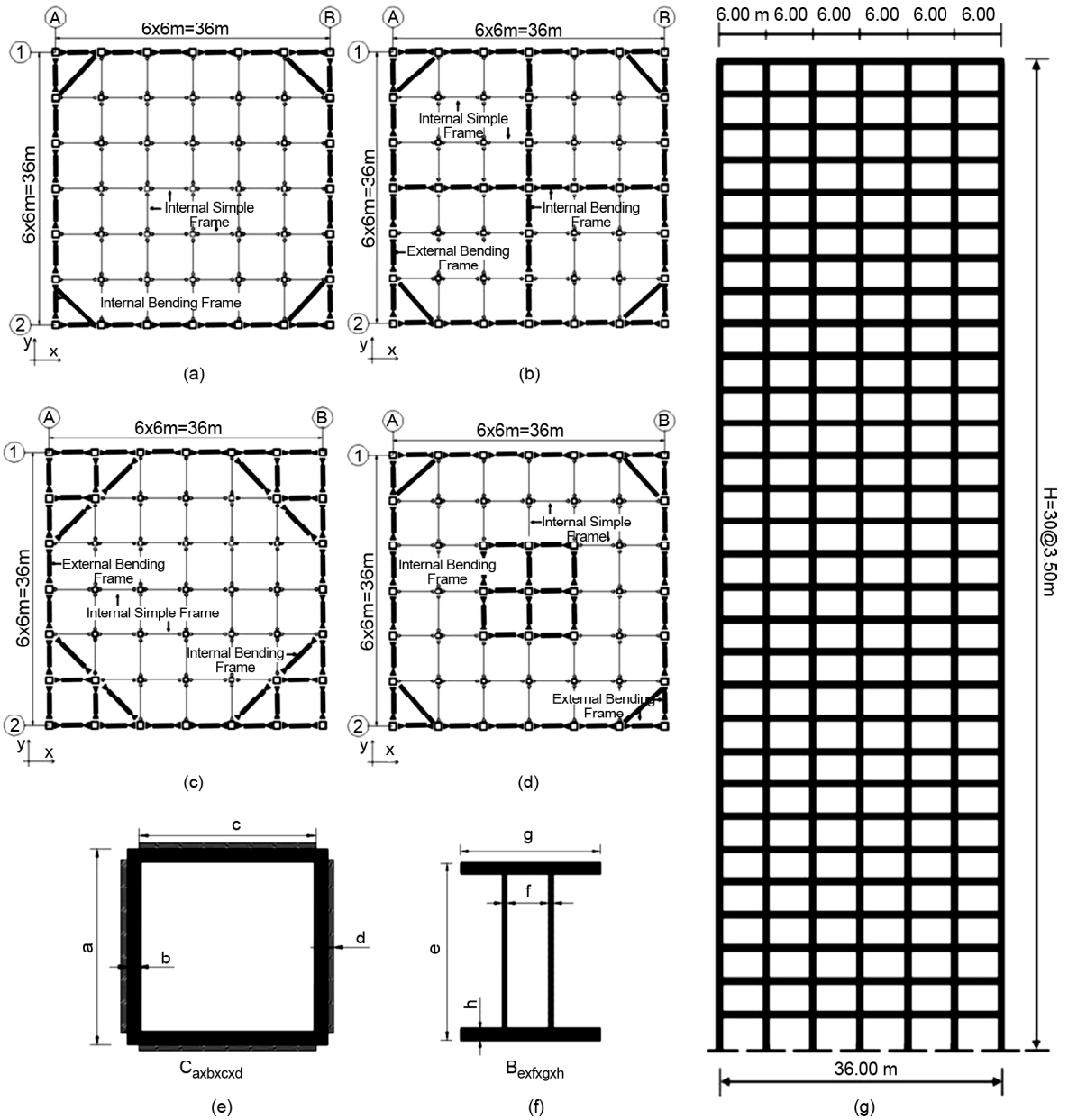

Figure 3. Structural models: (a) Plan of framed tube (F.T.); (b) Plan of bundled tube (B.T.); (c) Plan of castled tube (Ca.T.); (d) Plan of cellular tube (Ce.T.); (e) Columns section property of the 30-story models; (f) Beams section property of the 30-story models; (g) Structure view.

Table 2. The structural members of the 30-story studied models (mm).

Stories Groups	Interior Columns (Pinned Bents)	Interior and Exterior Columns (Rigid Bents)	Beams (Rigid Bents)
1-5	C550x30	C750x30x650x25	B500x20x500x25
6-10	C500x25	C700x30	B500x20x500x25
11-15	C450x25	C650x30	B500x20x500x25
16-20	C400x25	C600x30	B500x20x450x25
21-25	C350x20	C550x25	B450x20x400x25
26-30	C300x10	C500x15	B350x15x400x20

4. The Ensemble of Chosen Earthquake Records

The ensemble of selected earthquake records in this research includes seven near and far-field ones which contain various tectonic occurrences. The main physical characteristics of chosen records cover a wide range of frequency content, strong ground motions duration and various high seismological amplitudes. The maximum peak ground acceleration and velocity obtained from Table (3) are 0.999g and 167 cm/sec respectively, both are high values.

Generally, peak ground velocity (PGV) is often viewed as a better indicator of damage potential than peak ground acceleration (PGA). However, velocity time histories of some records listed in Table (3) are shown in Figure (4). The large velocity pulses evident in the plots would be viewed as damaging features. However, the damage potential also depends on how much dynamic ground displacement occurs during these velocity pulses.

The main physical characteristics of chosen records are shown in Table (4). The velocity time history diagram of the chosen near-field records and a number of their seismological characteristics of the chosen earthquake records are also illustrated in Figure (4).

It has to be mentioned that in this research, seismic response parameters of the studied structural models are analyzed and assessed in the Y direction of the plan (Figure 3).

Table 3. Results of the maximum roof acceleration (g is the gravity acceleration).

Structural Model (Figure 3)	F.T.	B.T.	Ca.T.	Ce.T
Max. Floor Acceleration	1.120g	1.050g	1.070g	1.080g
Amplification Coefficient	1.310	1.230	1.250	1.260

4.1. The Codified Hysteretic Loop

The four buildings described in the earlier section are numerically evaluated though employing non-linear dynamic time history procedures to assess

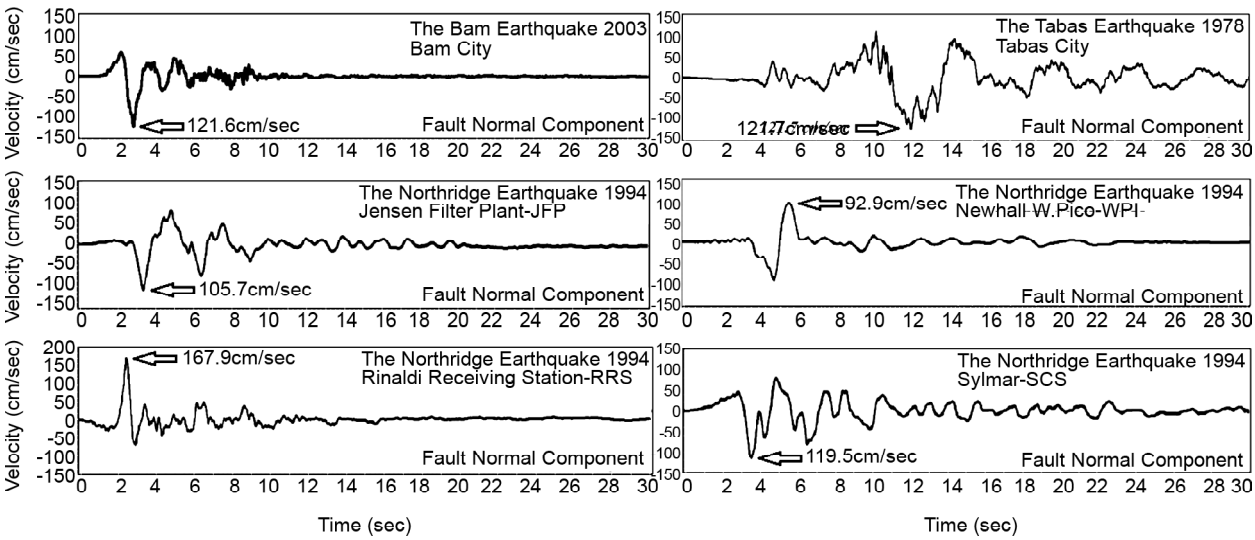

Figure 4. Ground velocity time histories from Table (1) containing high-amplitude coherent velocity pulses [11].

Table 4. Selected earthquake records.

Ground Motion	Component	Duration (sec)	PGA (g)	PGV (cm/s)	PGD (cm)	Magnitude (M_W)	PGV/PGA (sec)	PGD/PGV (sec)
Tabas 1978 Tabas City - 3.0 km	LN	30.00	0.836	97.7	39.9	7.4	0.12	0.40
	TR		0.851	121.3	94.5		0.14	0.78
	UP		0.688	45.5	17.0		0.06	0.37
Bam 2003 Bam City - 1.0 km	I.N	30.00	0.635	59.6	20.7	6.6	0.09	0.34
	TR		0.793	123.7	37.4		0.16	0.30
	UP		0.999	37.66	10.11		0.03	0.26
Northridge 1994 Sylmar (SCS) - 6.40 km	LN	30.00	0.897	102.23	45.28	6.7	0.11	0.44
	TR		0.612	117.47	54.16		0.19	0.46
	UP		0.586	34.59	25.63		0.06	0.74
Northridge 1994 Newhall (WPI) - 7.10 km	LN	30.00	0.325	67.40	16.10	6.7	0.21	0.23
	TR		0.455	92.80	56.60		0.20	0.61
	UP		0.290	37.20	13.30		0.13	0.35
Northridge 1994 Jensen Filter Plant (JFP) -6.10 km	LN	30.00	0.593	99.10	23.96	6.7	0.16	0.24
	TR		0.424	105.95	50.69		0.25	0.47
	UP		0.399	33.91	8.89		0.08	0.26
Northridge 1994 Rinaldi (RRS) - 7.10 km	LN	30.00	0.472	72.72	19.82	6.7	0.15	0.27
	TR		0.838	166.87	29.79		0.19	0.17
	UP		0.852	51.01	11.71		0.06	0.22
Northridge 1994 Moor-Park (MPR) – 28.00 km	LN	30.00	0.193	20.11	4.49	6.7	0.1	0.22
	TR		0.292	20.50	4.65		0.07	0.22
	UP		0.159	7.80	0.89		0.05	0.11

Fault Parallel: LN, Fault Normal: TR, Fault Vertical: UP

the resulting structural demands. Based on FEMA reports 356 and 440, in order to describe the non-linear behavior of beams and columns in the modeling process of the studied structures, the nonlinear hinge M3 as well as the nonlinear hinge P-M2-M3 are applied for all beams and columns of the planar rigid frames respectively [36-37]. The schematic nonlinear behavior of the noted hinges is illustrated in Figure (5). These default properties can be implemented numerically in well-known CSI computer software i.e. SAP2000 and Perform 3D, which are used in this research [38-39].

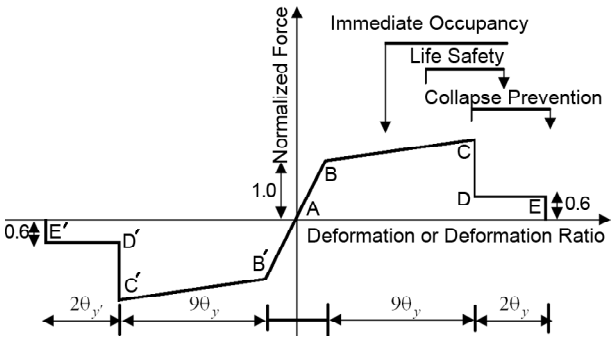

Figure 5. The FEMA analytical model for nonlinear behavior of beam-column element [11].

5. Assessment of the Results

The mentioned analyses have been accomplished by the use of the Newmark-beta integration method through the average acceleration criteria (the Newmark method $\gamma=0.50$ and $\beta=0.25$) [40-41]. The illustrated analytical results include the graphs, related to envelop maximum amounts of obtained structural responses parameters. The noted seismic structural response indicators, sequentially include the seismic base shear, absolute acceleration, relative velocity, the maximum dynamic displacement of all floor levels as well as the seismic drift demand of each level, as well as the configuration of plastic hinge, shear lag phenomena and residual drift.

In graphs related to the absolute acceleration, relative velocity, maximum displacement and drift of floor levels, the perpendicular axis shows the story number. Moreover, the horizontal axis sequentially belongs to the envelop maximum of the afore-mentioned response parameters. The response parameters for all 30-story models are illustrated in Figures (6) to (12). The calculated maximum seismic base shears and the static base shear that has been considered in the designation of the studied models are presented in Figure (6). According to the

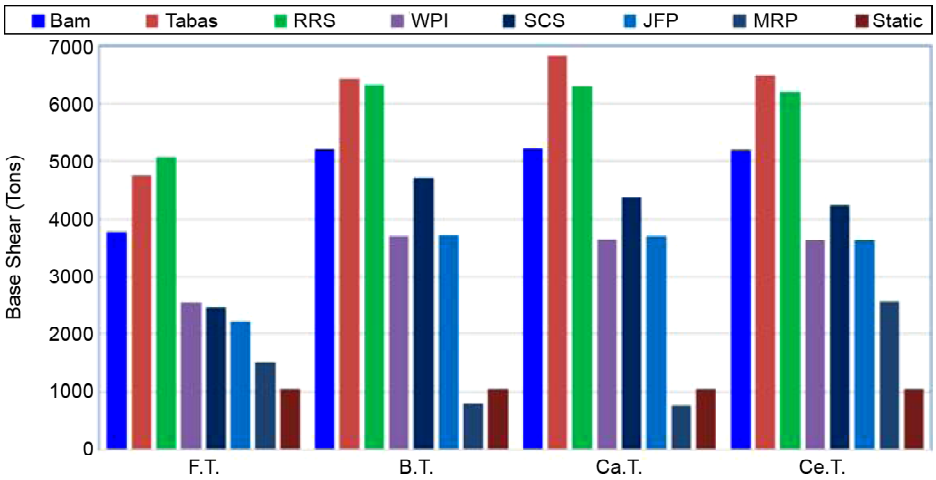

Figure 6. The maximum seismic base shear caused by the records as well as the static criterion.

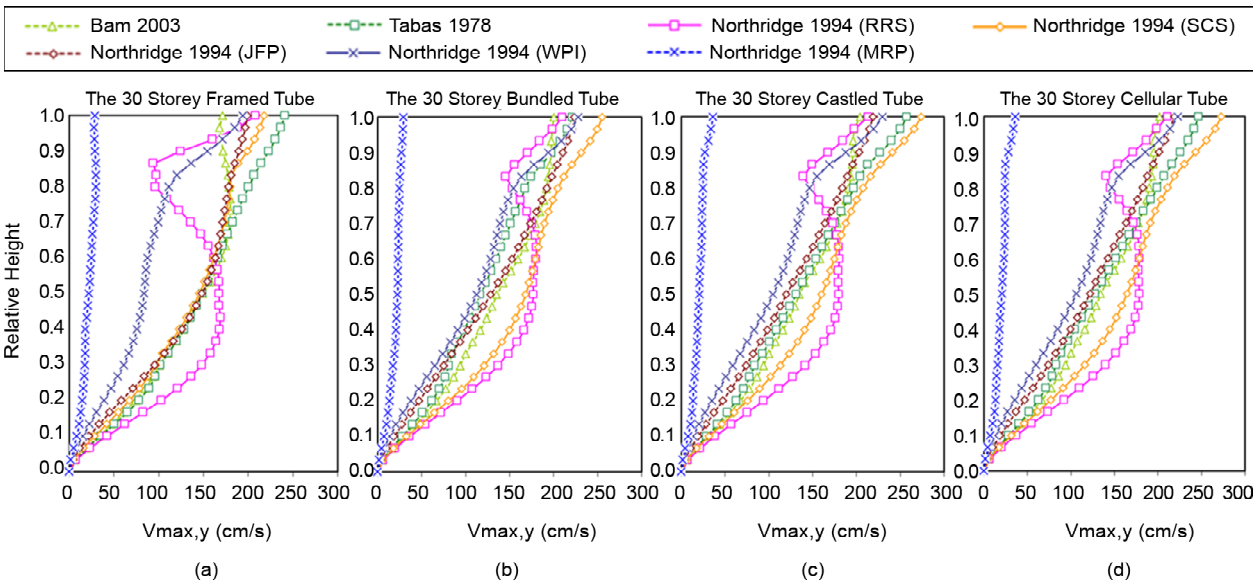

Figure 7. The envelop of stories maximum velocity of, (a) The 30-story F.T.; (b) The 30-story B.T.; (c) The 30-story Ca.T.; (d) The 30-story Ce.T.

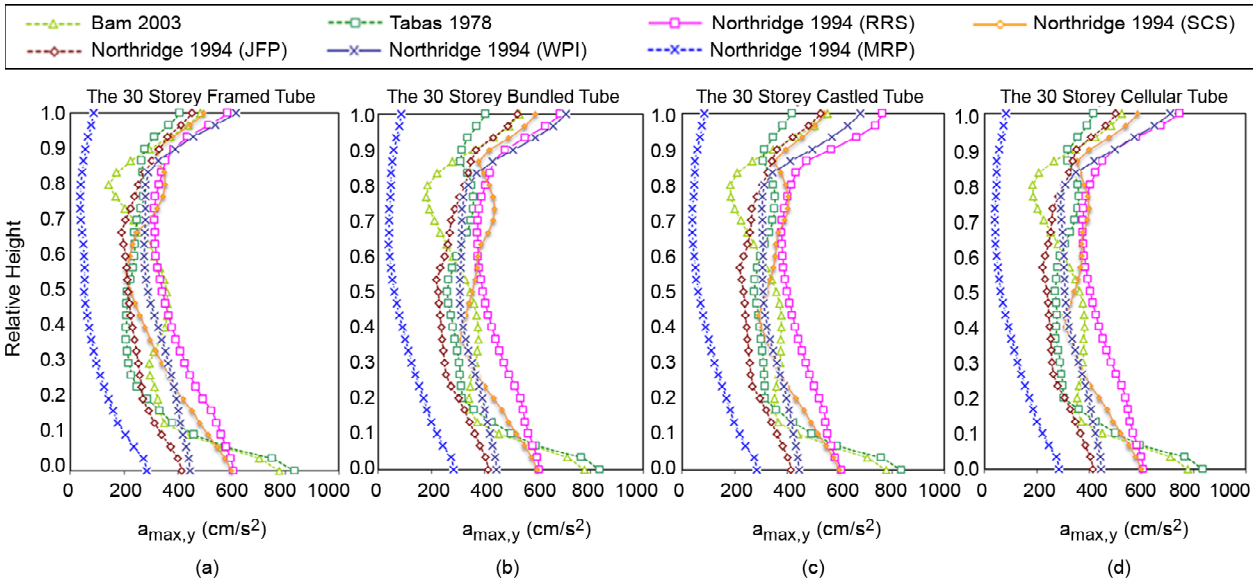

Figure 8. The envelop of stories maximum acceleration of, (a) The 30-story F.T.; (b) The 30-story B.T.; (c) The 30-story Ca.T.; (d) The 30-story Ce.T.

presented results, it is confirmed for the structural models which are affected by near-field earthquake records, the obtained base shears are relatively higher than those ones subjected to the far-field earthquakes.

The envelop curves of maximum absolute acceleration and relative velocity of floor levels of four different studied framed tube arrangements are presented in Figures (7) and (8). The obvious results of this process are the distribution of acceleration and velocity demands to floor levels at distinctly higher amounts, as compared to the ones resulted from far-field records. The envelop curves of maximum drift demands, obtained from the performed

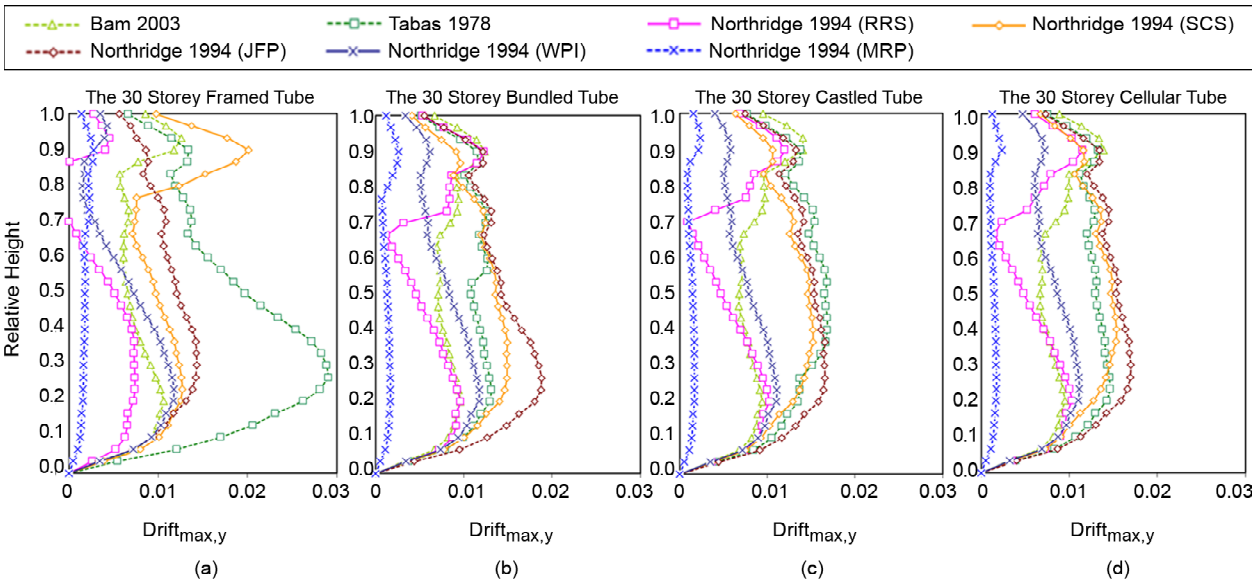

Figure 9. The envelop of stories maximum drift of, (a) The 30-story F.T.; (b) The 30-story B.T.; (c) The 30-story Ca.T.; (d) The 30-story Ce.T.

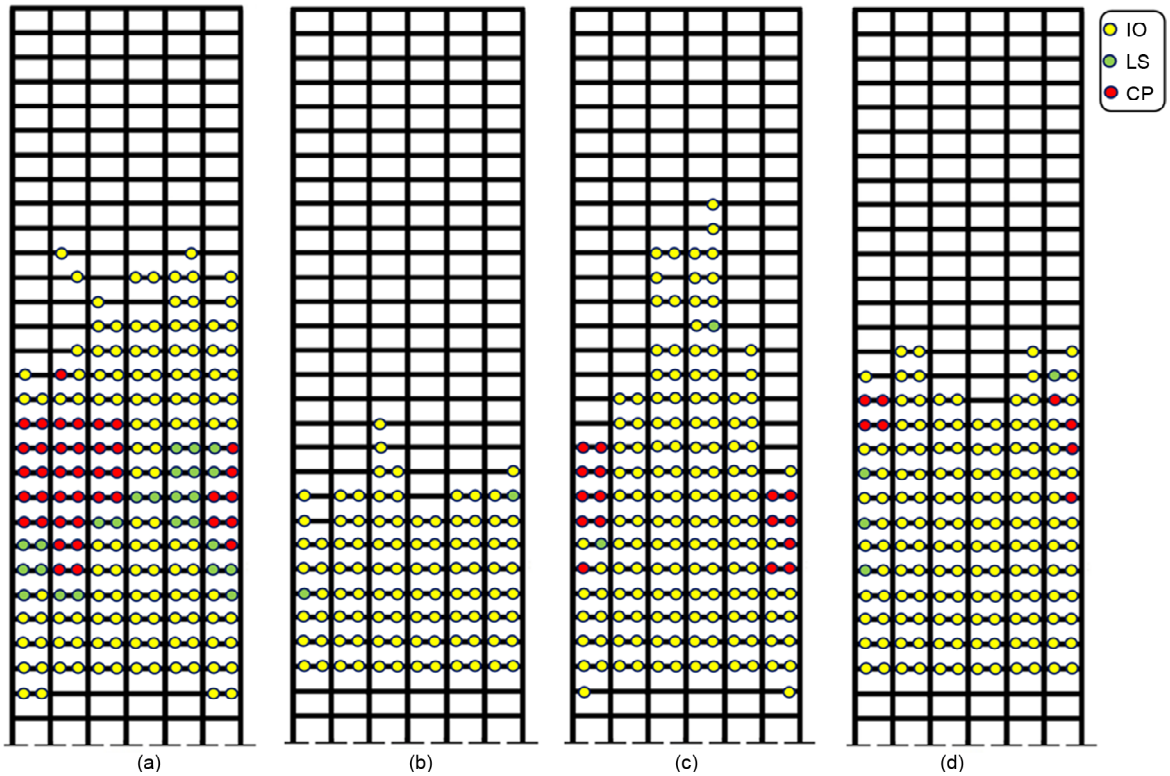

Figure 10. The maximum codified seismic rotation and corresponding plastic hinge caused by the Tabas record in fame 1 located in Y direction of plan: (a) The 30-story F.T.; (b) The 30-story B.T.; (c) The 30-story Ca.T.; (d) The 30-story Ce.T.

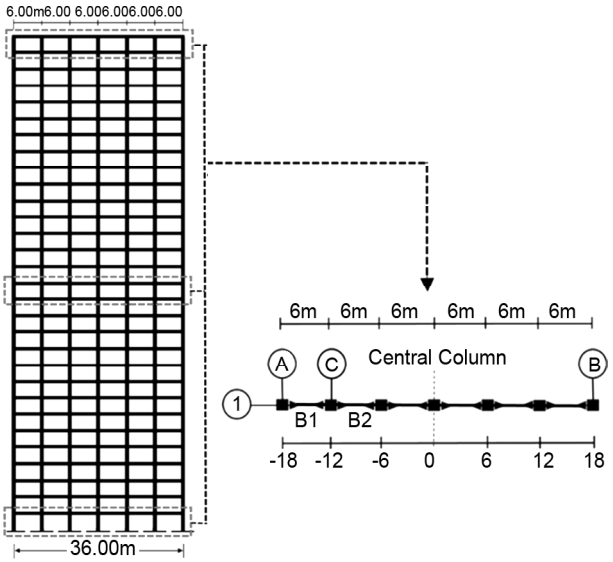

Figure 11. Arrangement of evaluated columns in frame 1 at the base, middle and top levels of the studied 30-story model.

nonlinear time history analyses under the records of Table (4) are shown in Figure (9). Analytical results prepared through applied near-fault records that contain pulse features show a remarkable increase in the calculated amounts of drift demands of the studied models.

Maximum drift demand in B.T., Ca.T. and Ce.T. models are generated by the JFP record that creates a relative displacement less than 2%, and the maximum drift in F.T. caused by the Tabas record is about 3%. Meanwhile, the near-fault records impose extremely higher demands than far-fault records. Moreover, the maximum drift is generally concentrated at the middle and upper stories levels. Furthermore, the distinct result caused by this phenomenon would also be a wide distribution of plastic hinges along with great amounts of drift parameter on the whole body of resistant structural skeleton. The maximum drift demands are mainly focused in lower and mid-levels of four studied models while for F.T. these demands reach their maximum amount in these levels as shown in Figure (10).

As follows, by drawing the models façade in the Y direction of the plan and displaying the formation of the plastic mechanism on it subjected to the Tabas record, the detailed visualization of different dissipation processes of earthquake kinetic energy can be observed, which are influenced by the first large period modes of vibrations (Figure 10a).

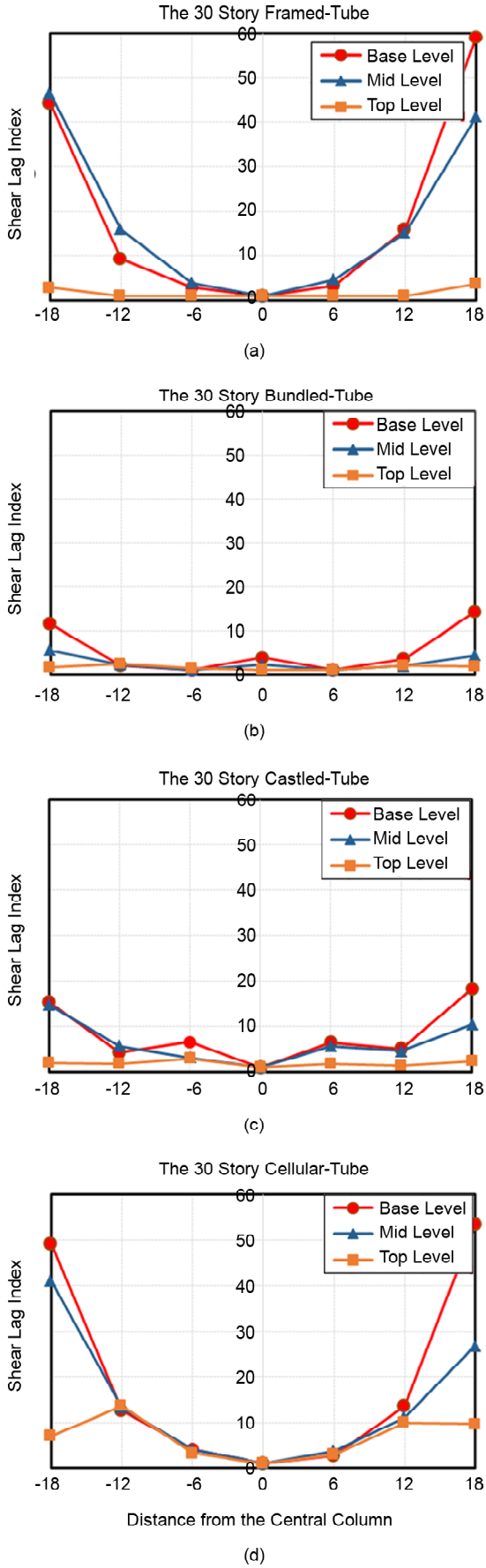

Figure 12. The shear lag index diagram resulted from axial forces envelope along the height of structure in columns of frame 1 (Figure 11): (a) The 30-story F.T.; (b) The 30-story B.T.; (c) The 30-story Ca.T.; (d) The 30-story Ce.T.

5.1. Shear Lag Phenomenon

The dynamic shear lag effect causes a nonlinear distribution of axial stresses across the sides of the structure plan, which is commonly found in box girders under lateral load. This effect results in higher stresses at the corner columns than the inner columns of the sides. Besides, by changing inner rigid frame arrangement in the plan of framed tube systems as well as the position of the transfer floor in the height of building, it becomes possible to optimize the seismic behavior of these structures and reduce the occurrence of shear lag effects. Hence, there is the opportunity of decreasing the consumption of total materials, along with maintaining the desirable qualities of the seismic design.

A number of seismic response parameters of the studied structures including the shear lag effects, at three selected levels of the building's basement, middle and top, resulting from nonlinear dynamic analyses are shown in Figure (12). In order to conduct a detailed and parametric analysis of the shear lag effects, the studied models are assessed at the three mentioned floor levels. In this regard, a non-dimensional parameter is defined as the shear lag index. The shear lag index is assumed as the ratio of each column's axial force in the intended axis to the middle column's axial force, i.e. the central column in the side rigid frame. In these graphs, the vertical row indicates the relative shear index, and the horizontal row indicates the columns in which this index is studied. The arrangement of analyzed columns in the side frame (columns in a flange chord) is portrayed in Figure (3).

It is noticed that in Figure (12), the graphs of the column's shear lag index in Figure (11) are shown at three reference levels of the base, middle and top situations of the height which are selected in all four studied models. Results indicate axial forces' average envelope in columns of Figure (11) subjected to a set of six near-field records. Noticeable points in the aforementioned graphs show that the maximum shear lag index in 30-story studied models with the basic tube frame at three reference levels of the building's base, middle and top are respectively, resulted as 59, 45 and 4 as illustrated in Figure (12-a). This is while the same results obtained for the bundled tube frame are 15, 5 and 1.5, for the castle tube frame are 18, 16 and 2, and finally for the cellular tube frame the results equal 53, 41 and 12, as displayed in Figures (12-b, c and d). The maximum of this index for a bundled tube system equals 15 and, for the castle tube frame equals 18, which show a respective decrease of about 75% and 70% compared to the basic framed tube in Figures (12-b and c).

Another detailed study of response parameter was accomplished on the residual drift under strong Tabas record. As observed in Figure (13-a), the percentage of persistent drift has reached to approximately 1.5% for the basic framed tube structure. Apart from the basic framed tube model in Figure (3), the other framed tube systems have shown a noticeable decrease in the domain of residual nonlinear displacements after the occurrence of strong earthquakes. As displayed in Figure (13-b, c, d), for all three structural models, this parameter is less than 1% at its highest value in the castled tube, and less than 0.5% in the cellular tube and bundled tube, which reveal a decrease over 70%.

Figure (14) shows the time history of the floor acceleration under the Tabas record. Table (4) lists the maximum values of the floor acceleration in relation with the PGA of the Tabas 1978 record, i.e. 0.852g. However, the noted acceleration amplification coefficient is the ratio of maximum roof acceleration to the PGA parameter of 0.852g.

The numerical results are corresponding to the Y direction of the plan (Figure 3). According to the results, it is observed that the rate of variation of the maximum roof acceleration for all four 30-story studied models, has a relatively high value. The calculated amplification coefficients for all four structural models are less than 1.31. This factor is at its highest value for the 30-story F.T. and less than 1.31 for the companion studied models Ce.T., B.T. and Ce.T., too. It reveals a decrease of about 6%, comparatively. Moreover, a significant and measurable response parameter to assess the structures seismic performance is maximum relative displacement, i.e. drift of floor levels. These numerical results are obtained according to the conducting of nonlinear dynamic analyses for all the studied framed tube arrangements as shown in Figure (15).

A precise review of Figure (15) denote that both of the Ca.T. and B.T. models can generally display higher structural efficiency with a decreasing process in the domain. Additionally, the rate of displacement variations, especially in the upper floors

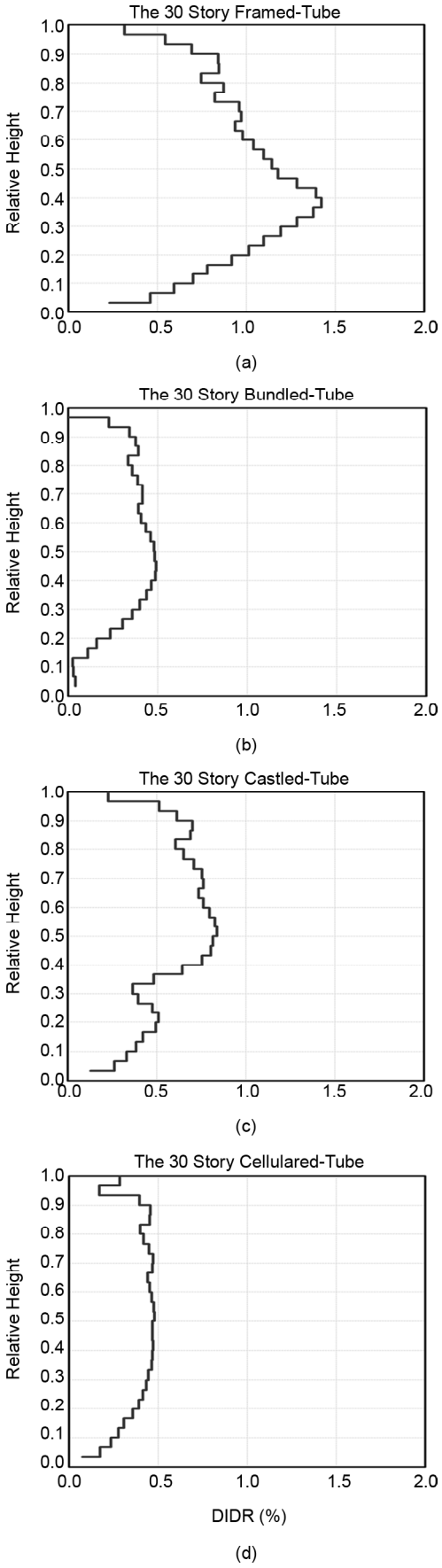

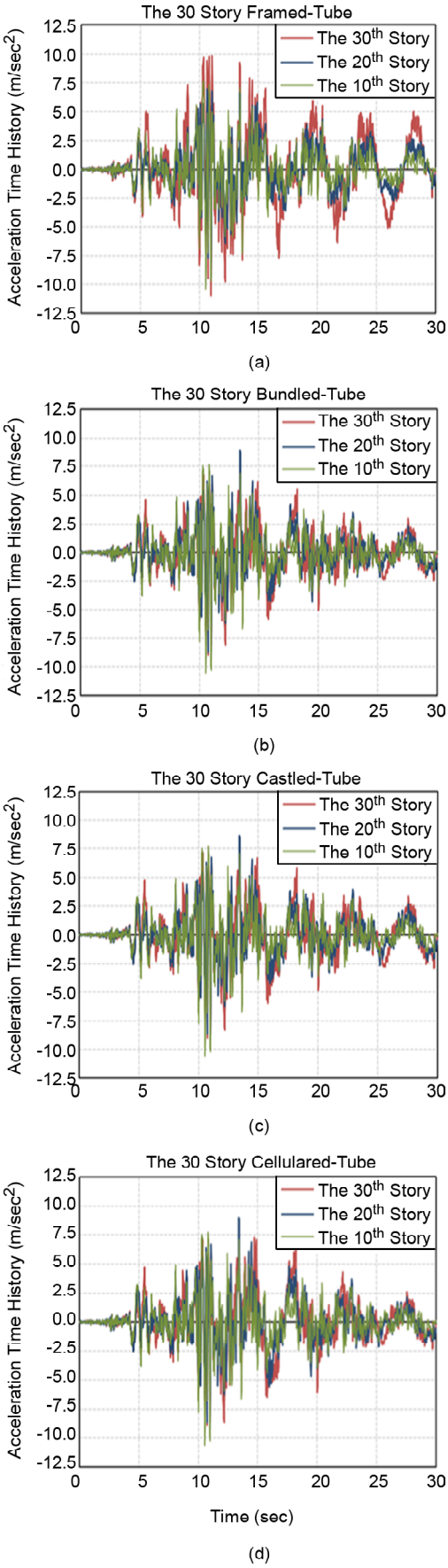

Figure 13. The height-wise distribution of residual (permanent) inter-story drift demand under Tabas near-fault seismic sequences: (a) The 30-story F.T.; (b) The 30-story B.T.; (c) The 30-story Ca.T.; (d) The 30-story Ce.T.

Figure 14. The floor acceleration time history subjected to the Tabas record in Y direction of plan at three notified levels of the studied models (Figure 3): (a) The 30-story F.T.; (b) The 30-story B.T.; (c) The 30-story Ca.T.; (d) The 30-story Ce.T.

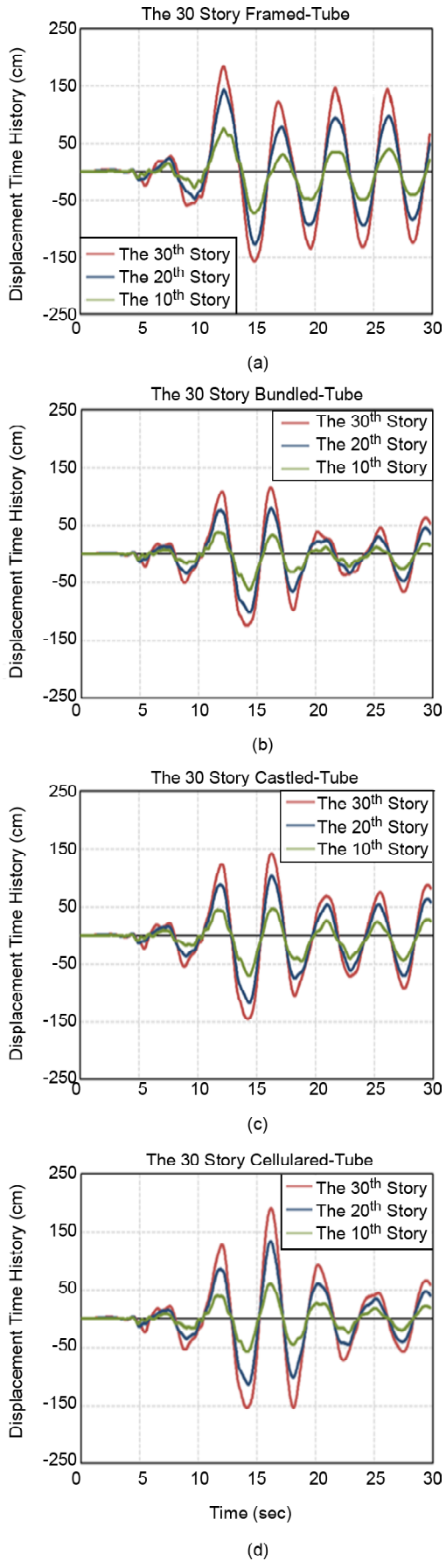

Figure 15. The floor displacement time history subjected to the Tabas record in Y direction of plan at three notified levels of the studied models (Figure 3): (a) The 30-story F.T.; (b) The 30-story B.T.; (c) The 30-story Ca.T.; (d) The 30-story Ce.T.

of the studied models, has the same manner. Meanwhile, these two mentioned resistant systems contain a few more rigid frames and panelized bents than the F.T. structure. It is apparent that the 30 story B.T. and Ca.T. models represent about 65% and 30% reduction in the roof displacement parameter as compared to the F.T. model.

6. Conclusions

The major goals in this presented research are describing important parameters and special characteristics of the near-fault ground motions as well as their effects on the dynamic responses of steel framed tube based structural systems. Nevertheless, the results of this study show that large velocity pulses displayed in the time history of the energized near-field records related to the Northridge earthquake 1994, can impose severe inelastic demands in the seismic response parameters of high-rise steel structures. Furthermore, the general drift demand is less than 0.02 in three of the studied models except the F.T. model. However, the maximum value for velocity of stories is greater than 250 cm/sec in the Y direction of the plan of the studied models.

The existence of compound or hybrid rigid frame structures in the interior arrangement of framed tube structures can result in a remarkable decrease in the inconsistency of dynamic axial stress, specially in corner columns and a decline in seismic shear lag effects. It is worthy of mention that studying the changes in the arrangement of inner rigid frames in compound framed tube structures is for the purpose of reaching a suitable arrangement for resistant systems and also reduce the structure requirements such as drift, base shear, axial stress, shear lag effect, plus the formation process of plastic hinges at the building's height, which have not been as much analyzed and researched so far.

The obtained results indicate the fact that a decent arrangement and bundled configuration of interior rigid frames could remarkably reduce the appearance of dynamic shear lag phenomenon in the overall seismic behavior of compound framed-tube skeletons. The maximum of the shear lag index for the bundled tube and castled tube systems, equals to 15 and 18 respectively. This manner shows a reduction almost up to 75% and 70% as compared to the corresponding result relating to the basic framed tube.

References

1. Taranath, B.S. (2005) *Wind and Earthquake Resistant Buildings Structural Analysis and Design*. Department of Civil and Environmental Engineering Georgia Institute of Technology, Atlanta, Georgia.

2. Naeim, F. (2001) *The Seismic Design Handbook*. 2nd Edition, Kluwer Academic Publisher.

3. Coull, A. and Bose, B. (1975) Simplified analysis of frame-tube structures. *Journal of Structural Division*, **101**, 2223-2240.

4. Azad, A., Ngo, T., and Samali, B. (2015) Control of wind-induced motion of tall buildings using smart façade systems. *Electronic Journal of Structural Engineering*, **14**(1), 33-40.

5. Choi, S.W., Seo, J.H., Lee, H.M., Kim, Y., and Park, H.S. (2015) Wind-induced response control model for high-rise buildings based on resizing method. *Journal of Civil Engineering and Management*, **21**(2), 239-247.

6. Elawady, A.K., Okail, H.O., Abdelrahman, A.A., and Sayed-Ahmed, E.Y. (2014) Seismic behavior of high-rise buildings with transfer floors. *Electronic Journal of Structural Engineering*, **14**(2), 57-70.

7. Kwok, K.C.S., Tse, K.T., and Campbell, S. (2011) Field measurements of dynamic properties of high-rise buildings. *Advances in Structural Engineering*, **14**, 1107-1128.

8. Ali, M.M. and Moon, K.S. (2007) Structural developments in tall buildings: Current trends and future prospects. *Architectural Science Review*, **50**(3), 205-223.

9. Gunel, M. Ilgin, M.H. (2007) A proposal for the classification of structural systems of tall buildings, *Building and Environment*, **42**(7), 2667-26.

10. Coull, A. (1988) Methods of analysis in the design of tall concrete and masonry buildings. *Council on Tall Buildings and Urban Habitat*, 921-944.

11. Azhdarifar, M. (2015) *Assessment of Seismic Response Parameters of Tall Buildings with Bundled Tube Structural System Subjected to Strong Near-Field Earthquake Records*. M.Sc. Thesis, Kharazmi University.

12. Shin, M., Kang, T., and Pimentel, B. (2010) Towards optimal design of high-rise building tube systems. *The Structural Design of Tall and Special Buildings*, **21**(6), 447-464.

13. Zaghi, A.E., Soroushian, S., Itani, A., Maragakis, E.M., Pekcan, G., and Mehrraoufi, M. (2014) Impact of column-to-beam strength ratio on the seismic response of steel MRFs. *Bulletin of Earthquake Engineering*, **13**(2), 635-652.

14. Shahrouzi, M., Meshkat-Dini, A. and Azizi, A. (2015) Optimal wind resistant design of tall buildings utilizing mine blast algorithm. *International Journal of Optimization in Civil Engineering*, **5**(2), 137-150.

15. Azhdarifar, M. Meshkat-Dini, A. and Sarvghad Moghadam, A. (2015) Evaluation of seismic response of tall buildings with framed tube skeletons in high seismic areas. *Proceedings of the 7th International Conference on Seismology and Earthquake Engineering* (SEE7), Tehran, Iran.

16. Somerville, P.G. (2003) Magnitude scaling of the near fault rupture directivity pulse. *Physics of the Earth and Planetary Interiors*, **137**(1-4), 201-212.

17. Mena, B. and Mai, P.M. (2011) Selection and quantification of near-fault velocity pulses owing to source directivity. *Georisk*, **5**(1), 25-43.

18. Ruzi Ozuygur, A. (2016) Performance-based seismic design of an irregular tall building - a case study. *Structures*, **5**, 112-122.

19. Azhdarifar, M., Meshkat-Dini, A., and Sarvghad Moghadam, A. (2015) Assessment of seismic response of mid-rise steel buildings with structural configuration of framed tube skeletons. *Proceedings of the 7th International Conference on Seismology and Earthquake Engineering* (SEE7), Tehran, Iran.

20. Erdik, M., Demircioglu, M.B., Sesetyan, K., and Harmandar, E. (2011) Characterization of long period strong ground motion. *Journal of Seismology and Earthquake Engineering*, **13**(1), 1-15.

21. Azhdarifar, M., Meshkat-Dini, A., and Sarvghad Moghadam, A. (2015) Study on the seismic response parameters of steel medium-height buildings with framed-tube skeleton under near-fault records. *Electronic Journal of Structural Engineering* (EJSE), **15**(1), 70-87.

22. Chanerley, A. and Alexander, N. (2010) Obtaining estimates of the low-frequency 'fling', instrument tilts and displacement time series using wavelet decomposition. *Bulletin of Earthquake Engineering*, **8**(2), 231-255.

23. Movahed, H., Meshkat-Dini A., and Tehranizadeh M. (2014) Seismic evaluation of steel special moment resisting frames affected by pulse type ground motions. *Asian Journal of Civil Engineering* (BHRC), **15**(4), 575-585.

24. Chioccarelli. E and Iunio Iervolino. (2010) Near-source seismic demand and pulse-like records: A discussion for L'Aquila earthquake. *Earthquake Engineering and Structural Dynamics*, **39**(7), 1039-1062.

25. Sofi, M., Hutchinson, G.L., and Duffield, C. (2015) Review of techniques for predicting the fundamental period of multi-story buildings: effects of nonstructural. *International Journal of Structural Stability and Dynamics Components*, **15**(2), DOI: http://dx.doi.org/10.1142/S0219455414500394.

26. Ghahari, S.F. and Khaloo, A.R. (2013) Considering rupture directivity effects, which structures should be named 'long-period buildings'. *The Structural Design of Tall and Special Buildings*, **22**(2), 165-178.

27. Hemmat, M., Hashemi, S.S., and Vaghefi, M. (2013) Seismic evaluation of steel frames subjected to decaying sinusoidal records through IDA method. *Journal of Seismology and Earthquake Engineering*, **15**(3-4), 207-222.

28. Alonso-Rodriguez, A. and Miranda, E. (2015) Assessment of building behavior under near-fault pulse-like ground motions through simplified models. *Soil Dynamics and Earthquake Engineering*, **79**, 47-58.

29. Ghahari, S.F., Moradnejad, H.R., Rouhanimanesh, M.S., and Sarvghad-Moghadam, A. (2013) Studying higher mode effects on the performance of nonlinear static analysis methods considering near-fault effects. *KSCE Journal of Civil Engineering*, **17**(2), 426-437.

30. Bray, J.D. and Rodriguez-Marek, A. (2004) Characterization of forward directivity ground motions. *Soil Dynamic and Earthquake Engineering*, **24**(11), 815-828.

31. Trifunac, M.D. and Todorovska, M.I. (2013) A note on energy of strong ground motion during Northridge, California, earthquake of January 17, 1994. *Soil Dynamics and Earthquake Engineering*, **47**, 175-184.

32. Baker, W.J. and Cornell, C. (2008) Vector-valued intensity measures for pulse-like near-fault ground motions. *Engineering Structures*, **30**(4), 1048-1057.

33. Mollaioli, F. and Bosi, A. (2012) Wavelet analysis for the characterization of forward-directivity pulse-like ground motions on energy basis. *Meccanica*, **47**(1), 203-219.

34. Standard No. 2800 (2014) Iranian code of practice for seismic resistant design of buildings, 4th Edition, Tehran, Iran.

35. Iranian National Building Code (Steel Structures - Division 10), Tehran, Iran (2014).

36. FEMA 356, Federal Emergency Management Agency (1998).

37. FEMA 440, Improvement of Nonlinear Static Seismic Analysis Procedures, Applied Technology Council (ATC-55 Project) (2005).

38. CSI (2010) Analysis reference manual for Sap2000, Berkeley-California, USA.

39. CSI (2007) PERFORM3D - structural analysis / software, Berkeley-California, USA.

40. Chang S.Y. (2003) Accuracy of time history analysis of impulses. *Journal of Structural Engineering*, ASCE, **129**(3), 357-372.

41. Miranda, I., Ferencs, R.M., and Hughes, T.J.R. (1989) An improved implicit-explicit time integration method for structural dynamics. *Earthquake Engineering and Structural Dynamics*, **18**(5), 643-653.